

## Flow and Motion of a Six Degree of Freedom Robot Manipulator

T.Rajasanthosh kumar<sup>1</sup>, K.suresh babu<sup>2</sup>, Dr.ch.mallikarjuna<sup>3</sup> D.V Srikanth<sup>4</sup>

<sup>1</sup>(Department of mechanical engineering, College/ University Name, Country Name) (10 Italic)

<sup>2</sup>(Department, College/ University Name, Country Name) (10 Italic)

---

**Abstract:** In this article, a methodology to finish pick-and-place operations utilizing a six level of-opportunity (DOF) automated arm connected to a wheeled portable robot is introduced. This examination work is a piece of a greater venture in building up a mechanical helped nursing to be utilized as a part of medicinal settings. The noteworthiness of this venture depends on the expanding interest for elderly and handicapped gifted care help which these days has turned out to be inadequate. Solid endeavors have been made to consolidate innovation to satisfy these necessities.

A few techniques were actualized to make a 6-DOF controller equipped for performing pick-and-place operations. Some of these strategies were utilized to accomplish particular errands, for example, taking care of the reverse kinematics issue, or arranging an impact free way. Different techniques, for example, forward kinematics portrayal, and workspace assessment, were utilized to depict the controller and its abilities. The controller was precisely depicted by acquiring the connection change lattices from each joint utilizing the Denavit-Hartenberg (DH) documentations. An Iterative Inverse Kinematics technique (IIK) was utilized to discover different arrangements for the controller along a given way. The IIK strategy depended on the particular geometric normal for the controller, in which a few joints share a typical plane. To discover permissible arrangements along the way, the workspace of the controller was considered. Logarithmic definitions to acquire the particular workspace of the 6-DOF controller on the Cartesian arrange space were gotten from the solitary designs of the controller. Nearby adroitness examination was likewise required to recognize conceivable introductions of the end-effectors for particular Cartesian facilitate positions..

**Keywords:** 6-DOF- Inverse Kinematics technique (IIK) - Logarithmic definitions

---

### I. Introduction

To move a protest starting with one place then onto the next utilizing a versatile robot, route and movement control of the robot are required. This examination, as a component of a noteworthy venture, is centered around the movement control of a six level of-flexibility (6-DOF) robot controller connected to a wheeled portable robot. A legitimate clarification on how the controller was picked is introduced. This record contains reproduction and trial aftereffects of an undertaking planned to outline and actualize a calculation for movement of an automated controller to fulfill pick-and-place operations. Such operations must be performed keeping away from stationary hindrances found in an indoor room condition. The diverse methodologies actualized to accomplish the previously mentioned assignments in a 6-DOF controller are depicted in this examination

### II. Objective

1. To accurately describe the robotic arm configuration in order to compute the forward kinematics equations.
2. To effectively solve the inverse kinematics problem with minimum computational effort.
3. To define the entire workspace of the manipulator (interior and exterior boundaries) in order to design paths with reachable configurations.
4. To select an adequate end-effector orientation for any specific coordinate position so that possible configurations of the manipulator are found.
5. To design a collision-free path to avoid stationary obstacles.
6. To evaluate the effectiveness of the proposed method by comparing simulation

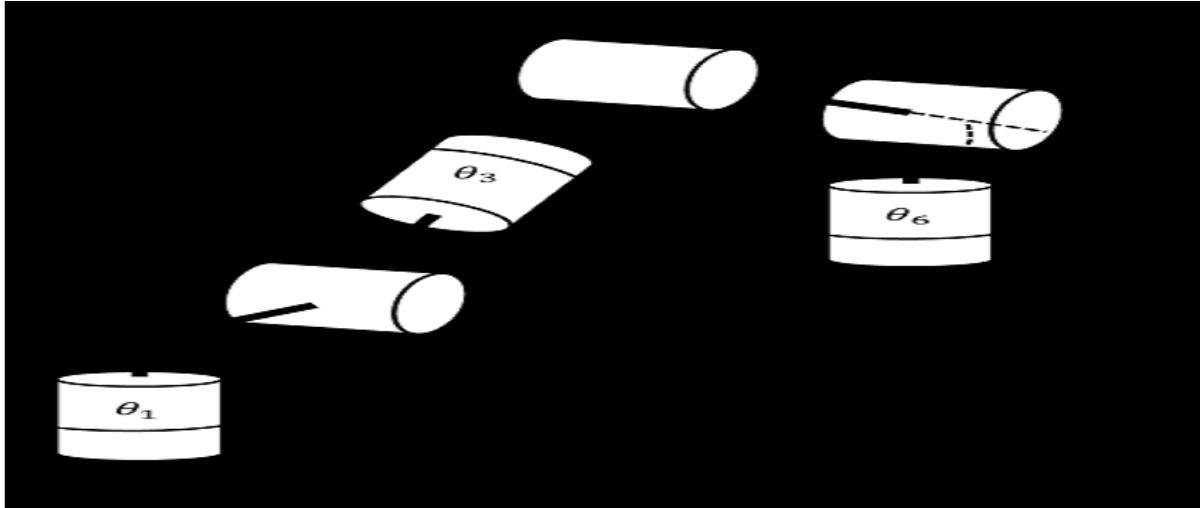


Fig 1 6-DOF manipulator -Wheeled mobile robot

### III. Problem Description and Analysis

Pick-and-place operations can be performed by isolating such operations into a few errands to be illuminated separately. The accompanying errands and their answers are clarified in this section: 1) inferring forward kinematics conditions in light of the portrayal of the controller, 2) taking care of the reverse kinematics issue, 3) figuring of the workspace the controller and its portrayal in the Cartesian facilitate framework, 4) deciding the end-effector introduction, 5) outlining a worldwide way to maintain a strategic distance from zones inside the workspace where the controller has movement control challenges.

### IV. Manipulator Description

The 6-DOF automated arm utilized as a part of this task is a serial chain controller made out of a few modules and a gripper end-effector interconnected by six revolute joints as introduced in Figure 3. The previously mentioned modules can be squared or round and hollow units as appeared in Figure 3.a. Every module has a worked in brushless servomotor equipped for conveying torque of 372Nm on the squared units and 239Nm on the tube shaped units. The most extreme speed came to by the modules is 8.2 rad/s for the squared units and 1.2 rad/s for the round and hollow units. Such modules additionally contain incremental encoders for situating and speed control and have completely incorporated power and control hardware. These modules are fit for pivoting more than 360 degrees yet have dividing constraints because of the controller setup.

Joint	Lower Limit	Upper Limit
1	-160°	160°
2	-120°	95°
3	-160°	160°
4	-119°	119°
5	-119°	119°
6	-180°	180

Table I: The 6-DOF robotic arm joint limits

Frame (i)	$a_{i-1}$	$a_{i-1}$	$d_i$	$\theta_i$
1	0	0	$l_1$	$\theta_1$
2	-90°	$l_2$	0	$\theta_2-90^\circ$
3	-90°	0	$l_3$	$\theta_3$
4	-90°	0	0	$\theta_4-90^\circ$
5	0	$l_4$	0	$\theta_5+90^\circ$
6	-90°	0	$-l_5$	$\theta$

Table II: Denavit-Hartenberg parameters

The investigation is started by picking the joint point limits, as appeared in Table I, to abstain from hitting the controller itself. All modules were instructed with a Controller Area Network (CAN) correspondence framework. Albeit a few programming capacities exist to control the robot controller, just certain capacities were actualized

Put body of the paper here. Put body of the paper here.

paper here. Put body of the paper here.

To keep the underlying position design as the home position as appeared in Figure 3, in which all the joint edges are zero, the joint factors ( $\theta_i$ ) were balanced  $+90^\circ$  or  $-90^\circ$  as appeared in Table II. Considering the previously mentioned modification and in light of

Craig's tradition the homogenous change that relates the end-effector position and introduction with the worldwide arrange framework is given

$${}^0T_6 = {}^0T_1 {}^1T_2 {}^2T_3 {}^3T_4 {}^4T_5 {}^5T_6 = \begin{bmatrix} r_{11} & r_{12} & r_{13} & p_x \\ r_{21} & r_{22} & r_{23} & p_y \\ r_{31} & r_{32} & r_{33} & p_z \\ 0 & 0 & 0 & 1 \end{bmatrix}$$

where,

$$r_{11} = c_6 [c_{45}(s_1 s_3 + c_1 s_2 c_3) - s_{45} c_1 c_2] - s_6 [s_1 c_3 - c_1 s_2 s_3]$$

$$r_{21} = s_6 [c_1 c_3 + s_1 s_2 s_3] - c_6 [c_{45}(c_1 s_3 - s_1 s_2 c_3) + s_{45} s_1 c_2]$$

$$r_{31} = c_6 (s_{45} s_2 + c_{45} c_2 c_3) + c_2 s_3 s_6$$

by

$$r_{13} = -s_{45}(s_1 s_3 + c_1 s_2 c_3) - c_{45} c_1 c_2$$

$$r_{23} = s_{45}(c_1 s_3 - s_1 s_2 c_3) - c_{45} s_1 c_2$$

$$r_{33} = c_{45} s_2 - s_{45} c_2 c_3$$

$$p_x = l_2 c_1 + l_3 c_1 c_2 + (l_5 s_{45} + l_4 s_4)(s_1 s_3 + c_1 s_2 c_3) + (l_5 c_{45} + l_4 c_4)(c_1 c_2)$$

$$p_y = l_2 s_1 + l_3 s_1 c_2 - (l_5 s_{45} + l_4 s_4)(c_1 s_3 - s_1 s_2 c_3) + (l_5 c_{45} + l_4 c_4)(s_1 c_2)$$

$$p_z = l_5 (s_{45} c_2 c_3 - c_{45} s_2) + l_4 (c_2 c_3 s_4 - c_4 s_2) - l_3 s_2 + l_1$$

$$r_{12} = -s_6 [c_{45}(s_1 s_3 + c_1 s_2 c_3) - s_{45} c_1 c_2] - c_6 [c_3 s_1 - c_1 s_2 s_3]$$

$$r_{22} = s_6 [c_{45}(c_1 s_3 - s_1 s_2 c_3) + s_{45} s_1 c_2] + c_6 [c_1 c_3 + s_1 s_2 s_3]$$

$$r_{32} = c_2 s_3 c_6 - s_6 (s_{45} s_2 + c_{45} c_2 c_3)$$

$$r_{12} = -s_6 [c_{45}(s_1 s_3 + c_1 s_2 c_3) - s_{45} c_1 c_2] - c_6 [c_3 s_1 - c_1 s_2 s_3]$$

$$r_{22} = s_6 [c_{45}(c_1 s_3 - s_1 s_2 c_3) + s_{45} s_1 c_2] + c_6 [c_1 c_3 + s_1 s_2 s_3]$$

$$r_{32} = c_2 s_3 c_6 - s_6 (s_{45} s_2 + c_{45} c_2 c_3)$$

All the joint factors utilized as a part of Equation 4 were measured as for the home position as appeared in Figure 8. The documentation  $rij$  in Equation 4 speaks to the components of pivot framework, and  $p_{ij}$  the components of the position vector,  $c_i$  remains for  $\cos(\theta_i)$ ,  $s_i$  for  $\sin(\theta_i)$ ,  $c_{ij}$  for  $\cos(\theta_i + \theta_j)$ , and  $s_{ij}$  for  $\sin(\theta_i + \theta_j)$ .

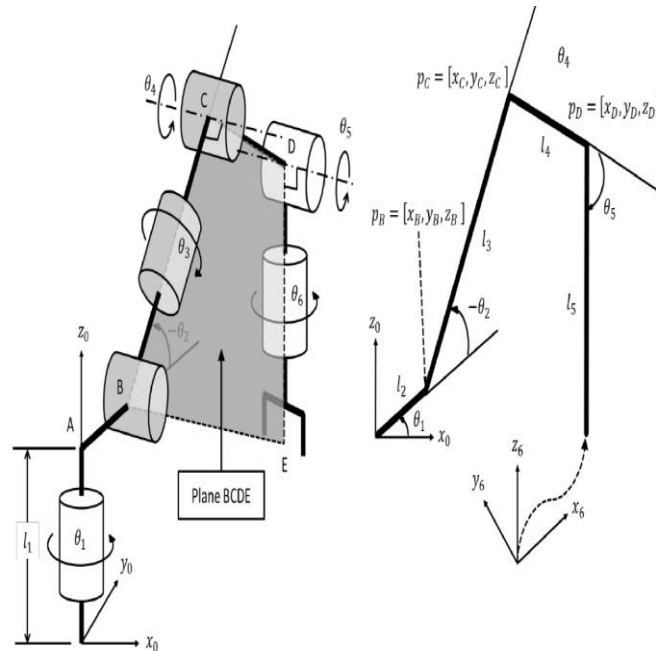
**Iterative Inverse Kinematics**

The Iterative Inverse Kinematics (IIK) technique proposed in this exploration comprised of inferring two synchronous non-straight conditions in view of the geometrical design of the controller. Such conditions can be inferred as far as the first and second joint points  $\theta\theta_1$  and  $\theta\theta_2$  of the controller. With respect to any reverse kinematics technique, the position and introduction of the end-effector are known. In the wake of finding the two concurrent conditions, the issue turns into that of tackling an arrangement of two nonlinear conditions. The underlying foundations of this arrangement of conditions speak to the arrangements, which are figured utilizing a bisecting technique. When joint edges  $\theta\theta_1$  and  $\theta\theta_2$  are ascertained, joint point 4 is processed utilizing the Law of cosines. The staying joint edges are figured utilizing kinematics conditions from Equation .

*Calculating joint angles  $\theta_1$  and  $\theta_2$*

To acquire two synchronous conditions, the geometrical setup of the controller is considered. The robot controller is demonstrated in the Cartesian organize framework to break down its geometrical arrangement as appeared in Figure 4. Letters A, B, C, D and E are doled out to every controller joint to recognize its position. Since the pivot tomahawks at joints C and D are parallel to each other and, the portions BC and ED are both ordinary to these revolution tomahawks, it can be gathered that the focuses B, C, D and E are in one plane paying little heed to the joints points an incentive as appeared in Figure 4.

The past proclamation determined into the accompanying articulation  
 $:[EDXDC] \cdot BC = 0$



**.4 Schematic diagram of the 6-DOF Manipulator: (a) Plane BCDE; (b) Vector form**

positions of points  $p_B$  and  $p_C$  can be expressed as:

$$p_B = [(l_2 c_1)(l_2 s_1) 0]$$

$$p_C = [(l_2 c_1 + l_3 c_2 c_1)(l_2 s_1 + l_3 c_2 s_1)(-l_3 s_2)]$$

the following expression for the first simultaneous equation is obtained:

$$(r_{23} z_D - r_{33} y_D) c_2 c_1 + (r_{33} x_D - r_{13} z_D) c_2 s_1 + (r_{23} x_D - r_{13} y_D) s_2 + r_{13} l_2 s_1 s_2 - r_{23} l_2 c_1 s_2 = 0$$

Solving for  $\theta_2$  in above Equation the following expression is obtained:

$$\tan(\theta_2) = (r_{23} z_D - r_{33} y_D) c_1 + (r_{33} x_D - r_{13} z_D) s_1 \pm [(r_{23} x_D - r_{13} y_D) + r_{13} l_2 s_1 - r_{23} l_2 c_1]$$

$$x_D = p_x - r_{13} l_5$$

$$y_D = p_y - r_{23} l_5$$

$$zD=pz-l1-r33l5$$

The second simultaneous equation is found by computing the length of the segments *BC* and *DC*. The magnitudes of these segments are known as they are the offset links parameters from table I. The following equation was obtained:

$$BC+DC-l3-l4=0$$

the following error nonlinear equation  $|E|$  is computed as:

$$|E|=xD2+yD2+zD2+l22+l32-l42-2(l2+l3c2)(xDc1+yDs1)+2l3(zDs2+l2c2)$$

The change of sign over a particular interval represents a zero crossing, and suggested the existence of a solution. An iteration process was done at these intervals to obtain an accurate result.

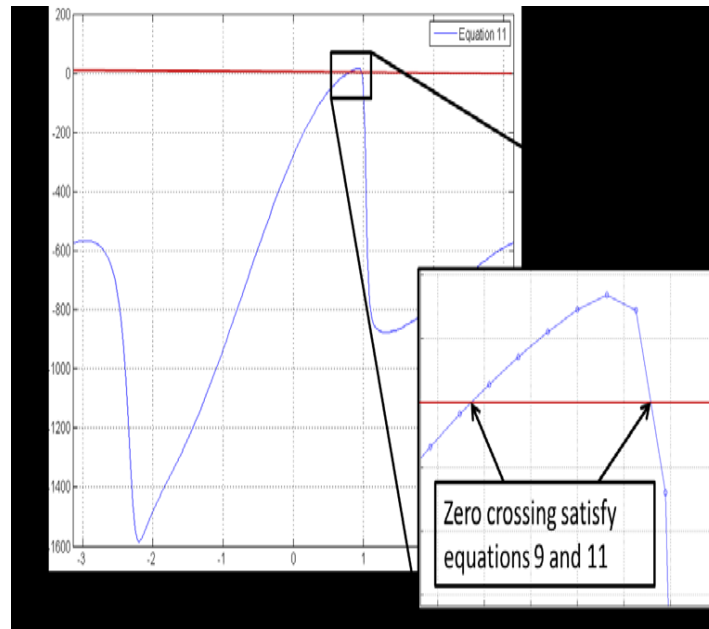


Fig 4 Finding the roots for equation  $|E|$

To stay away from misdetection when finding the underlying foundations of long interims greatest and least length mistake  $|E|$  were ascertained and included into the joint edge  $\theta_1$  set. It was discovered that the base mistake happened when joint edge  $\theta_1$  was arranged toward the end-effectors. The most extreme mistake happened when joint edge  $\theta_1$  was arranged to the inverse side.

$$min=atan2(py,px)$$

$$max=atan2py,\pm\pi$$

The atan2 work processes the point framed between the x and y parts given considering its esteems as well as its signs

**Calculating joint angle  $\theta_4$**

Using the Law of Cosines on the triangle formed by A, B and C in figure4,  $\theta_4$  was calculated as:

$$c4=xD2+yD2+zD2+l22-l32-l42-2l2(xDc1-yDs1)/2l3l4$$

$$s4=\pm(1-c42)^{0.5}$$

$$\theta4=atan2(s4,c4)$$

Two unique designs were gotten per each  $\theta_1$  arrangement as appeared in Equation above. This conduct, as expressed by Gudric ,permitted coordinate control more than a few designs. In this specific case, elbow-up or elbow-down could be picked.

**Calculating joint angle  $\theta_3$**

Considering that the position vector of the fifth joint,  $xD$ , and  $zD$  parameters, are known from Equation, the following transformation is implemented:

$${}^0_5T = {}^0_2T {}^2_5T$$

the dependence of the joint angles  $\theta_1$  and  $\theta_2$  was transferred to the left hand side, obtaining the following equation:

$${}^0_2T^{-1} = \begin{bmatrix} c_1s_2 & s_1s_2 & c_2 & -l_1c_2 - l_2s_2 \\ c_1c_2 & s_1c_2 & -s_2 & l_1s_2 - l_2c_2 \\ -s_1 & c_1 & 0 & 0 \\ 0 & 0 & 0 & 1 \end{bmatrix}$$

$${}^2_5T = \begin{bmatrix} c_3c_{45} & -c_3s_{45} & -s_3 & l_4c_3s_4 \\ -s_{45} & -c_{45} & 0 & l_4c_4 + l_3 \\ -s_3c_{45} & s_3s_{45} & -c_3 & -l_4s_3s_4 \\ 0 & 0 & 0 & 1 \end{bmatrix}$$

$$(T_{20}^{-1}T_{50})_{34} = c_1yD - s_1xD = -l_4s_3s_4 = T_{5234}$$

Then,  $\theta_3$  is obtained as:

$$s_3 = s_1xD - c_1yD / l_4s_4$$

$$c_3 = \pm(1 - s_3^2)^{0.5}$$

$$\theta_3 = \text{atan2}(s_3, c_3)$$

As before, two different configurations are obtained for  $\theta_3$ . Combining  $\theta_3$  and  $\theta_4$  solutions, four different configurations per  $\theta_1$  solution are found.

Calculating joint angle  $\theta_5$

transferring  $\theta_1$  and  $\theta_2$  to the left hand side we have

$$[T_{20}(\theta_1, \theta_2)]^{-1}T_{60} = T$$

$${}^0_2T^{-1} = \begin{bmatrix} c_1s_2 & s_1s_2 & c_2 & -l_1c_2 - l_2s_2 \\ c_1c_2 & s_1c_2 & -s_2 & l_1s_2 - l_2c_2 \\ -s_1 & c_1 & 0 & 0 \\ 0 & 0 & 0 & 1 \end{bmatrix}$$

$${}^0_6T = \begin{bmatrix} r_{11} & r_{12} & r_{13} & p_x \\ r_{21} & r_{22} & r_{23} & p_y \\ r_{31} & r_{32} & r_{33} & p_z \\ 0 & 0 & 0 & 1 \end{bmatrix}$$

$$r_{13}c_1s_2 + r_{23}s_1s_2 + r_{33}c_2 = -c_3s_4s_5$$

$$r_{13}c_1c_2 + r_{23}s_1c_2 - r_{33}s_2 = -c_4s_5$$

Thus,  $\theta_5$  is then obtained as:

$$s_4s_5 = r_{13}c_1s_2 + r_{23}s_1s_2 + r_{33}c_2 / -c_3$$

$$\theta_5 = \text{atan2}(s_4s_5, c_4s_5) - \theta_4$$

Calculating joint angle  $\theta_6$

the known joints on the left hand side, the following equation is obtained:

$$[T_{50}(\theta_1, \theta_2, \theta_3, \theta_4, \theta_5)]^{-1}T_{60} = T_{65}$$

$$r_{11}(s_1c_3 - c_1s_2s_3) - r_{21}(c_1c_3 + s_1s_2s_3) - r_{31}(c_2s_3) = -s_6$$

$$r12(s1c3-c1s2s3)-r22(c1c3+s1s2s3)-r32(c2s3)=-c6$$

So we get  $\theta_6 = \text{atan2}(s6, c6)$

The different arrangements got with the IIK strategy speak to leeway over the single arrangement acquired with the Newton's technique when obstruction shirking is required. The basis to pick one arrangement among the others along a coveted way depends on the nearest setup to that picked in the past position, gave that the controller does not hit the obstruction.

**Computing the Jacobian matrix**

Considering the end-effector global position vector ( $G\theta$ ) for the 6-DOF manipulator extracted from Equation, the joint angle  $\theta_6$  does not affect such position:

$$G\theta = [px \ py \ pz]^T = [f1(\theta_1, \theta_2, \theta_3, \theta_4, \theta_5) \ f2(\theta_1, \theta_2, \theta_3, \theta_4, \theta_5) \ f3(\theta_2, \theta_3, \theta_4, \theta_5)]^T$$

where  $f1$ ,  $f2$  and  $f3$  are the Cartesian coordinate position function of joint angles  $\theta_1, \theta_2, \theta_3, \theta_4$  and  $\theta_5$  as shown in the following expressions:

$$f1(\theta_1, \theta_2, \theta_3, \theta_4, \theta_5) = l2c1 + l3c1c2 + (l5s45 + l4s4)(s1s3 + c1s2c3) + (l5c45 + l4c4)(c1c2)$$

$$f2(\theta_1, \theta_2, \theta_3, \theta_4, \theta_5) = l2c1 + l3c1c2 + (l5s45 + l4s4)(s1s3 + c1s2c3) + (l5c45 + l4c4)(c1c2)$$

$$f3(\theta_2, \theta_3, \theta_4, \theta_5) = l5(s45c2c3 - c45s2) + l4(c2c3s4 - c4s2) - l3s2 + l1$$

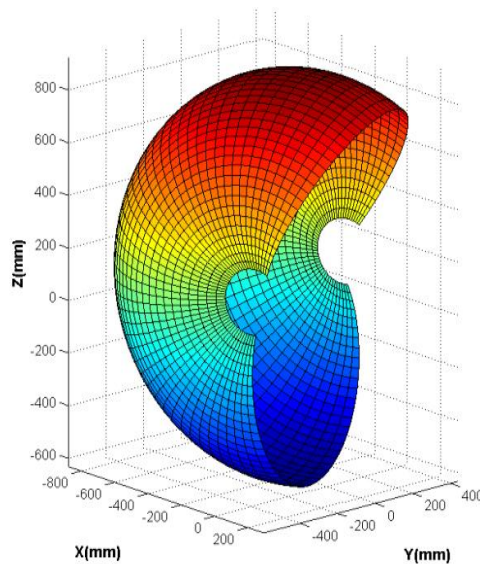
The Jacobian ( $J\theta$ ) can be then computed as:

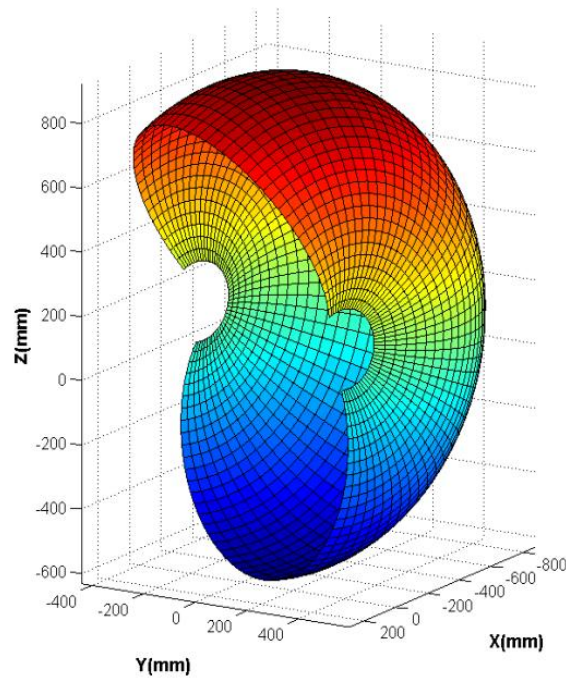
$$[D] = [J\theta][D\theta]$$

$$D = \begin{bmatrix} dpx \\ dpy \\ dpz \end{bmatrix}, \quad J_\theta = \begin{bmatrix} \frac{\partial f_1}{\partial \theta_1} & \frac{\partial f_1}{\partial \theta_2} & \frac{\partial f_1}{\partial \theta_3} & \frac{\partial f_1}{\partial \theta_4} & \frac{\partial f_1}{\partial \theta_5} \\ \frac{\partial f_2}{\partial \theta_1} & \frac{\partial f_2}{\partial \theta_2} & \frac{\partial f_2}{\partial \theta_3} & \frac{\partial f_2}{\partial \theta_4} & \frac{\partial f_2}{\partial \theta_5} \\ \frac{\partial f_3}{\partial \theta_1} & \frac{\partial f_3}{\partial \theta_2} & \frac{\partial f_3}{\partial \theta_3} & \frac{\partial f_3}{\partial \theta_4} & \frac{\partial f_3}{\partial \theta_5} \end{bmatrix}, \quad D_\theta = \begin{bmatrix} d\theta_1 \\ d\theta_2 \\ d\theta_3 \\ d\theta_4 \\ d\theta_5 \end{bmatrix}$$

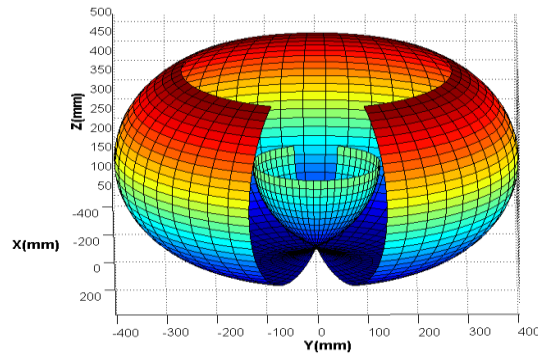
**Singular parametric surfaces**

In spite of the fact that up to eight joint designs can be found for particular positions and introductions of the end-effector for the 6-DOF automated arm, areas with solitary setup exist. Such particular arrangements are known as singularities and are portrayed by the loss of degrees of opportunity in the framework. The learning of these solitary arrangements is basic on the grounds that these setups may speak to the limit of the workspace, as well as areas in which the end-effector presents movement troubles. At the point when the controller achieves these solitary surfaces the end-effector development winds up noticeably constrained.

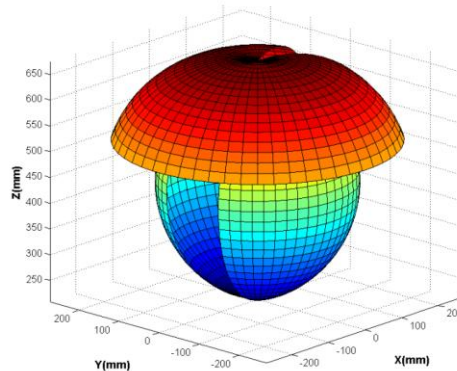




(B)



(C)



(D)

Singular parametric surfaces of the 6-DOF robot manipulator: a)  $G(s_2)$ ; b)  $G(s_3)$ ; c)  $G(s_{25})$ ; d)  $G(s_{28})$

## V. Conclusions

After analyzing the overall performance of the proposed algorithm, and comparing the simulation  
1. The joint edges of the controller were effectively ascertained at each position along the predefined ways utilizing the IIK presented here. The execution of this strategy was confirmed by getting every conceivable answer for every particular position of the end-effector. Such property enabled the controller to pick an

achievable answer for maintain a strategic distance from snags. The IIK technique turned out to be a reasonable strategy for taking care of the Inverse Kinematics issue.

2.The execution of the IIK strategy was contrasted and the execution of the pseudo-backwards Newton's technique. The computational endeavors per arrangement required to fathom the joint points utilizing the IIK technique were not exactly those required by the pseudo-backwards Newton's strategy

3.The examination of the workspace limits took into account the recognizable proof of the reachable purposes of the end-effector for the determination of the most fitting way. Despite the fact that a large portion of the parametric surfaces figured for the 6-DOF controller, don't constitute a limit for the workspace, they should be maintained a strategic distance from as they caused movement challenges in the controller.

### References

- [1]. J. Denavit and R. S. Hartenberg, "A Kinematic Notation for Lower-Pair Mechanisms based on Matrices", *Journal of Applied Mechanics*, Vol. 23, pp. 215-221, June 1955.
- [2]. J. J. Craig, "Introduction to Robotics: Mechanics and Control", 3rd edition, Prentice Hall, Upper Saddle River, N.J., USA, 2005.
- [3]. I. A. Vasilyev and A. M. Lyashin, "Analytical Solution to Inverse Kinematics Problem for 6-DOF Robot-Manipulator", *Automation and Remote Control*, Vol. 71, No. 10, pp. 2195-2199, 2010.
- [4]. M. Shimizu, H. Kakuya, W. K. Yoon, K. Kitagaki and K. Kosuge, "Analytical Inverse Kinematic Computation for 7-DOF Redundant Manipulators With Joint Limits and Its Application to Redundancy Resolution", *IEEE Transactions on Robotics*, Vol. 24, No. 5, pp. 1131-1142, 2008.
- [5]. C. W. Wampler, "Manipulator Inverse Kinematics Solution Based on Vector Formulations and Damped Least Squares Methods", *IEEE Transactions on Systems, Man, and Cybernetics*, Vol. 16, No. 1, pp. 93-101, 1986.
- [6]. S. R. Buss, J. S. Kim, "Selectively Damped Least Squares for Inverse Kinematics", *Journal of Graphics Tools*, Vol. 10, No. 3, pp. 37-49, 2005.
- [7]. G. Z. Grudic and P. D. Lawrence, "Iterative Inverse Kinematics with Manipulator Configuration Control", *IEEE Transactions on Robotics and Automation*, Vol. 9, No. 4, August 1993.
- [8]. D. Pieper and B. Roth, "The Kinematics of Manipulators Under Computer Control", *Proceedings of the Second International Congress of Theory of Machines and Mechanisms, Zaczopane, Poland*, Vol. 2, pp. 159-169, 1969.
- [9]. B. Siciliano, "A Closed-Loop Inverse Kinematic Scheme for Online Joint-Based Robot Control", *Robotica*, Vol. 8, No. 3, pp. 231-243, 1990.
- [10]. K. Abdel-Malek, H. Yeh and S. Othman, "Interior and Exterior Boundaries to the Workspace of Mechanical Manipulators", *Robotics and Computer Integrated Manufacturing*, Vol. 16, No. 5, pp. 365-376, 2000.
- [11]. K. Abdel-Malek and H. Yeh, "Analytical Boundary of the Workspace for General 3-DOF Mechanisms", *International Journal of Robotic Research*, Vol. 16, No. 2, pp. 198-213, 1997.
- [12]. K. Abdel-Malek and H. Yeh, "Geometric Representation of the Swept Volume using Jacobian Rank-Deficiency Conditions", *Computer Aided Design*, Vol. 29, No. 6, pp. 457-468, 1997.
- [13]. Niku, S., "Introduction to Robotics: Analysis, Systems, Applications", Prentice Hall, New Jersey, USA, 2001.
- [14]. K. Abdel-Malek and H. Yeh, "Local Dexterity Analysis for Open Kinematic Chains", *Mechanism and Machine Theory*, Vol. 35, No. 1, pp. 131-154, 2000.
- [15]. R. Fotouhi, H. Salmasi, I. Vaheed and M. Vakil, "Trajectory Planning for a Wheeled Mobile Robot and its Robotic Arm", *Proceedings of ASME 2010, International Mechanical Engineering Congress & Exposition, Vancouver, BC, Canada, November 12-18, 2010*.
- [16]. G. Ping, B. Wei, X. Li, X. Luo, "Real Time Obstacle Avoidance for Redundant Robot", *Proceedings of the 2009 IEEE, International Conference on Mechatronics and Automation, August 9-12, Changchun, China*, pp. 223-228, 2009.
- [17]. W. Zhang and T. M. Sobh, "Obstacle Avoidance for Manipulators", *Systems Analysis Modelling Simulation*, Vol. 43, No. 1, pp. 67-74, January 2003.
- [18]. Chien-Chou Lin, "A Hierarchical Path Planning of Manipulators Using Memetic Algorithm", *Proceedings of the 2009 IEEE, International Conference on Information and Automation, June 22-25, Zhuhai/Macau, China, 2009*.
- [19]. MathWorks®, Matlab® – Documentation Center (on-line): Surfaces, Volumes and Polygons: ellipsoid, Version 7.10 (R2010a), 2010.
- [20]. Schunk®, Amtec Robotics – Programmers guide for PowerCube™, Version 1.3, 2007.
- [21]. McGraw-Hill Professional, "McGraw-Hill Dictionary of Scientific and Technical Terms", 6th edition, McGraw-Hill, New York, USA, 2002.
- [22]. RoboWorks™, 3D Robot Modeling Software – Demonstration Version 3.0 <http://www.newtonium.com/>, January 7th 2012.